

Optical properties of ZnSe doped with Ag and Au

P. J. Dean

Royal Signals and Radar Establishment, St. Andrews Road, Malvern, Worcestershire, United Kingdom

B. J. Fitzpatrick and R. N. Bhargava

Philips Laboratories, Briarcliff Manor, New York 10510

(Received 7 December 1981; revised manuscript received 10 March 1982)

We present bound-exciton (BE) and donor-acceptor-pair (DAP) spectra of ZnSe grown by liquid-phase epitaxy and doped with the transition metals (TM) Ag and Au. Luminescence, luminescence excitation, and time decay spectra establish the assignments of the spectral features and show that Ag forms a medium deep acceptor, $(E_A)_{\text{Ag}} = 431 \pm 2$ meV, consistent with the activation energy for thermal quenching of the DAP spectra. This thermal technique, together with the less precise spectral measurements available for the more-strongly-phonon-coupled Au acceptor indicate that $(E_A)_{\text{Au}} \sim 550$ meV, appreciably less than the probable value for Cu, ~ 650 meV. Peculiarities in the BE properties within this TM sequence are discussed with reference to the influence of their *d*-state characteristics. Strong BE luminescence with no-phonon energy near 2.747 eV is attributed to a neutral $\text{Ag}_{\text{Zn}}\text{-Ag}_\text{I}$ associate, possibly a split interstitial. Reasons for its absence in ZnSe:Ag and ZnSe:Au are discussed. Isotope effects in this spectrum and that of the Li neutral acceptor BE are contrasted. The latter provides proof that Li_{Zn} is the persistent shallow T_d site acceptor in ZnSe. Further associate BE luminescence is tentatively identified for ZnSe:Ag and ZnSe:Au.

I. INTRODUCTION

Zinc selenide is a II-VI semiconductor of considerable current interest for a variety of optoelectronic applications, including displays, both in discrete-diode¹ and thin-film² forms. It is also of fundamental interest as the member of the II-VI family with probably the widest energy gap, yet retaining reasonably tractable crystal growth and doping control properties. Nevertheless, full control of the semiconducting properties of ZnSe has proved difficult. The search for controllable shallow acceptors has proved especially frustrating, although some recent progress has been made both in understanding and in realization.³

The present paper describes the fundamental behavior of the transition-metal (TM) dopants Ag and Au, which form acceptor-type cation substituents in II-VI semiconductors. They are best known in ZnS, where Ag is an activator of blue luminescence in an important class of cathode ray phosphors, P11, P22, etc. Kinetic studies establish-

ed that this luminescence is of distant donor-acceptor-pair (DAP) type,⁴ and recent detailed spectral analysis suggests $(E_A)_{\text{Ag}} \sim 0.72$ eV.⁵ This is much smaller than the value for Cu in ZnS (Table I) so that the ground-state wave function of the Ag acceptor is expected to contain a greater admixture of hostlike T_2 character from the "dangling bond" ligand states of the S anions.⁶ More recent photoluminescence spectra on ZnS:Ag thin films suggests that $(E_A)_{\text{Ag}}$ may be even lower, at ~ 0.56 eV. The summary data in Table I have been selected from the literature, with a bias towards those investigations in which the combination of crystal quality, types of measurement, and techniques of data analysis seem most likely to provide reliable information.

The extent to which TM-induced acceptor levels can be regarded as slightly and recognizably modified *d* states of the TM decreases rapidly with atomic number within the TM series for a given host⁶ and with increase in atomic number of the anion within a sequence of isoelectronic host crys-

TABLE I. Acceptor ionization energies E_A (meV). Footnotes denote acceptor ionization energies for Zn and Cd II-VI compounds. Trends: E_A increases with increase in atomic number of acceptor ion, E_A increases with decrease in atomic number of host site.

Compound	Acceptor								A Center ($V_{II}^{\bar{\bar{}}}-D^+$) ⁻
	Li _{II}	Na _{II}	Cu _{II}	Ag _{II}	Au _{II}	P _{VI}	As _{VI}	$V_{II}^{\bar{\bar{}}}$	
ZnO	~800 ^a	~600 ^b	3260 ^c						
ZnS	~150 ^{d,aa}	~190 ^d	1250 ^e	720 ^f					950 ^g
ZnSe	114 ^h	128 ^h	~650 ⁱ	430 ^j	550 ^j	85–90 ^{k,x}	~110 ^k	700 ^m	≤600 ^{n,y}
ZnTe	60.5 ^{o,p}	62.8 ^{o,p}	148 ^{p,q}	123 ^{o,p}	277 ^{o,p}	63.5 ^p	79 ^{o,p}		~700 ^{r,z,aa}
CdS	165±6 ^s	169±6 ^s	1100 ^t	260 ^u		120 ^{s,x}			
CdSe	109±6 ^t	109±6 ^t							
CdTe	60.7 ^v	61.7 ^w	149.5 ^w						

^aReference 59.

^bReference 60.

^cReferences 58 and 40.

^dReference 54.

^eReference 53.

^fReference 5.

^gReference 56.

^hReference 63.

ⁱReference 57.

^jPresent work.

^kReference 39.

^lReference 49.

^mThe microscopic nature of these centers is uncertain, but they are probably not simple substitutional centers.

ⁿEnergy shift of only ~40 meV between ($V_{II}^{\bar{\bar{}}}\text{Cl}_{VI}^+$)⁻ and ($V_{II}^{\bar{\bar{}}}\text{Al}_{II}^+$)⁻.

^oHere, the donor may be Zn_I⁺ in a close Frenkel pair.

^{aa}Hypothetical identification.

^mReference 50.

ⁿReference 51.

^oReference 9.

^pReference 10.

^qReference 46.

^rReference 52.

^sReference 45.

^tReference 55.

^uReference 61.

^vReference 47.

^wReference 48.

tals (Table I). In general, this is a consequence of variations of the relative positions of the host valence band and the TM atomic d states with the electronegativities of the atomic species involved. As is well known, the free atomic d states are modified by the influence of the host-crystal field, described by ligand-field spectroscopy,⁷ and by the nephelauxetic effect. This latter effect is relatively minor for the energy states of TM in wide-gap, strongly ionic hosts to which ligand-field theory has had greatest application. For more covalent hosts, the effect strongly modifies the values of the Racah parameters which characterize the electron-electron interaction within the free ion. For relatively covalent hosts, such as ZnTe within the Zn cation II-VI family, and for TM of large electronegativity, such as Cu, the strong hybridization between impurity d and host sp^3 bonding states reduces the fraction of d character of the levels in the host band gap so strongly that they closely approximate the states of main group acceptors. These states possess hostlike orbital characters and

relatively large orbital radii. They are well described by the familiar effective-mass theory of semiconductor physics, with significant deviations only for the *energy* of the lowest state.^{8–10}

The TM of interest in this paper, which have only a single hole in the d shell in their dominant atomic valence state, take on a closed-shell character in sufficiently covalent solids, and behave as classical main-group acceptor-type dopants. The contrasting electronic behaviors expected for TM impurities as their oxidation state is varied by alterations in the differential electron affinities between impurity and host have been discussed by Robbins and Dean.¹¹ The properties reported for the TM Ag and Au in the present paper can all be understood in terms of classical deep acceptorlike states where the impurity behaves as (A^-) h , with the (A^-) acceptorlike d^{10} core (M^+) rather than the open-shell isoelectronic case (A), with a d^9 core (M^{2+}). We shall see that the ground-state binding energies of these acceptors are large compared with the effective-mass-theory value which may be as

low as 80 meV in ZnSe.¹² Consequently, the representative points may lie near the right center of Fig. 1 of Robbins and Dean, consistent with the expected small positive differential electron affinities. Sharp structure caused by transitions between well-shielded *d* substates split by the crystal field, very characteristic of all TM in wide gap hosts, for example, Cu in ZnO (Ref. 13) or ZnS (Ref. 14), has not been reported for Ag and Au in ZnSe.

The TM Cu has properties comparable to Ag and Au but with slightly larger tendencies to form an open-shell configuration because of the greater electronegativity associated with lower atomic number within an isoelectronic sequence. We compare the energy positions of the deep acceptor states of Cu, Ag, and Au in the present paper (Table I). Discussion of more detailed properties, such as the *g* values obtained from Zeeman measurements, is reserved to a later paper. However, it is significant to observe here that the very unusual behavior observed for the ground-state *g* values of these TM in ZnSe but not ZnTe provides direct evidence of the significant hybridization with the TM *d* core expected for ZnSe from the above arguments.

Details of crystal preparation and techniques of optical characterization are presented in Secs. II A and II B. Bound exciton (BE) and DAP optical properties of ZnSe:Ag are presented and discussed in Secs. II A and III B, while similar properties of ZnSe:Au are presented in Secs. III C and III D. Finally, selectively excited photoluminescence (SPL) measurements, which firmly establish Li as the dominant shallow acceptor in ZnSe with T_d site symmetry, are reported in Sec. III E.

II. EXPERIMENTAL

A. Crystal preparation

The epitaxial layers were grown^{12,15} on wafers cut from substrate boules purchased from Eagle-Picher Industries, Inc. The nominal orientation of the wafers was [111]*A* (the Zn face). They were cleaned in solvents and etched in potassium hydroxide at 100°C for 15 sec. Several of the samples (including sample A) were grown in a horizontal reactor using a multichamber boat of the type used for the growth of (Ga,Al)As. The multichamber feature allowed for growth of undoped buffer layers, which helped to isolate the grown

layer from the substrate. A gold reflector furnace was used, in which the conventional base-metal winding was replaced by a platinum-rhodium winding in order to reduce contamination. A nitrogen-purged glove box surrounded the entry port to prevent atmospheric contamination. Tin (Kawecki Berylco, Inc.) was used as a solvent and Zn (Cominco, Inc.), selenium (MCP, Ltd.), and silver (Poly Research Corporation) were added as elements. The layers were grown by cooling from 920 to 830°C at 0.5 °C/min in a hydrogen atmosphere. Layer thickness in this system was between 5 and 10 μm.

Several other samples were grown in a vertical system in which all parts wetted by the melt were made of pyrolytic boron nitride. Bismuth (Cominco) was used as the solvent, and the layers were grown using a cooling rate of 1 °C/min over a similar temperature range. The thickness in these cases was about 25 μm.

The atom percent of silver was varied between 0.05% and 8.5% (the amount for sample A) in the melt, and gold (Engelhard) was varied between 0.004 and 0.4%. In the specific case of sample A, 0.04 mol % of Zn₃N₂ was also added. This improved the sharpness of the spectra, presumably due to the reduction of contaminants by reaction with *N*, without introducing any extraneous spectral features.

The same spectral features were seen in the case of both solvents, indicating that these features are not artifacts, but are truly due to the doping effects of the elements themselves. However, more silver was needed to achieve these same effects in the Sn case.

B. Techniques of optical measurements

The photoluminescence spectra were recorded photoelectrically using the calculator-controlled recording attachment at the focal plane of a 2m *f*/17 spectrograph reported earlier.¹⁶ Luminescence was excited either using ~360-nm light from a Kr⁺ laser or with continuously tunable light from a jet-stream-type dye laser with typical power levels of ~50 mW. Stilbene III dye was used to cover the energy range from ~2.71 to 2.82 eV. The crystals were cooled by direct immersion in liquid He, sometimes pumped below the λ point. High-resolution photoluminescence excitation (PLE) spectra were measured with the dye laser, using the spectrograph as a detector with the necessary degree of spectral resolution. Broader

energy range PLE spectra were measured with a 150-W lamp whose output was passed through a 1m $f/6$ grating monochromator and focused onto the sample through a filter to remove unwanted orders of exciting light and to reduce the stray-light level. The luminescence was focused directly onto an S20 photomultiplier through an appropriate filter with a sharp transition between long-wavelength transmission and short-wavelength absorption. Cathodoluminescence spectra were obtained with a square wave-modulated electron beam of energy ~ 20 keV and total current ~ 1 μ A, usually modulated with a 10% duty cycle.¹⁷ Lifetime measurements were made with this system, using a Biomation transient recorder with a system time resolution of about 50 nsec. The samples were cooled by attachment to the cold finger of a modified Oxford Instruments continuous-flow variable-temperature cryostat. This cryostat was capable of covering the temperature range 5–480 K necessary for the thermal-quenching measurements of all the spectra of interest. Luminescence was collected from the same irradiated face of the sample both in cathodoluminescence, using a focusing mirror with a small aperture at the pole to pass the electron beam with the sample mounted on a narrow cold finger near the focal point of the mirror,¹⁷ and in photoluminescence by taking the narrow exciting laser beam onto the crystal face in direct view of the spectrometer. In this way, the influence on the extrinsic luminescence components of the self-absorption effects of the epitaxial layer and of the much thicker and generally poorer optical quality ZnSe substrates was avoided. Both types of excitation penetrated only $\lesssim 2$ μ m of the sample surface, except in the DAP PLE measurements at energies well below the near-gap bound-exciton components.

III. EXPERIMENTAL RESULTS AND DISCUSSION

A. Bound-exciton luminescence of Ag-doped ZnSe

The near-gap luminescence of ZnSe:Ag (Figs. 1 and 2) is typical of lightly but inadvertently contaminated single crystals.^{16,18} Very weak free-exciton (FE) and donor-bound-exciton (DBE) components I_2 are observed, together with a strong additional component Ag_3 close to the energy of the Li acceptor bound exciton (ABE) (Sec. III E), but

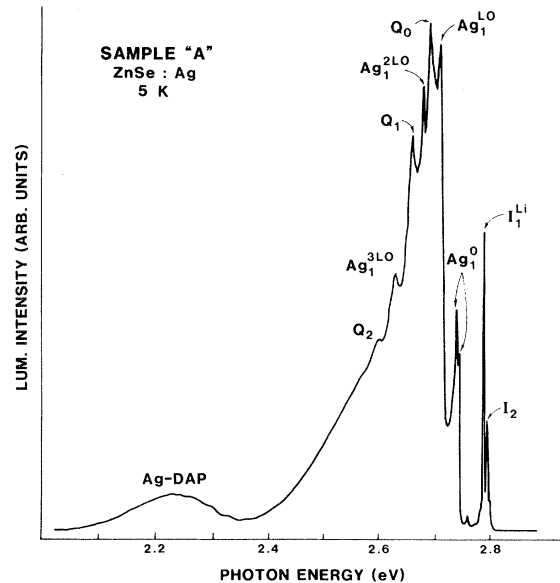


FIG. 1. Visible photoluminescence from a ZnSe:Ag single crystal recorded at low temperature under ~ 15 mW of focused 360-nm light from an Ar^+ laser. Components I_2 and I_1^{Li} are caused by recombination of excitons bound to shallow donors and Li acceptors. Q_0 contains no-phonon donor-acceptor-pair (DAP) luminescence involving the Li acceptor; Q_n are LO phonon replicas of Q_0 . The green DAP luminescence involving the deep Ag acceptor and the luminescence of BE at an Ag-related associate, no phonon components Ag_1 , are also present. It is believed that an Ag ABE Ag_3 is isoenergetic with I_1^{Li} .

with a distinctly smaller S parameter (Table II). The Huang-Rhys parameter S is a measure of the coupling to the particular phonon, here compared for the longitudinal-optical (LO) phonon which is a prominent feature in most electronic spectra in a significantly polar semiconductor such as ZnSe. The S parameter is defined by the intensity ratio of the one LO-phonon and no-phonon luminescence components, if the electron-phonon coupling can be described by the Frölich Hamiltonian.

Swaminathan and Greene¹⁹ (SG) have made the most extensive previous measurements on BE in ZnSe:Ag, with the use of melt-grown single crystals. They observe a new Ag-related BE at 2.7957 eV (their component Ag_1^0), just below the energy range of the usual DBE and therefore suggest the presence of a new donor, possibly the interstitial Ag_I . We also observe an unusual line in this region, labeled Ag_4^0 in Fig. 2, seen particularly clearly for excitation just below the FE energy E_{GX} . The

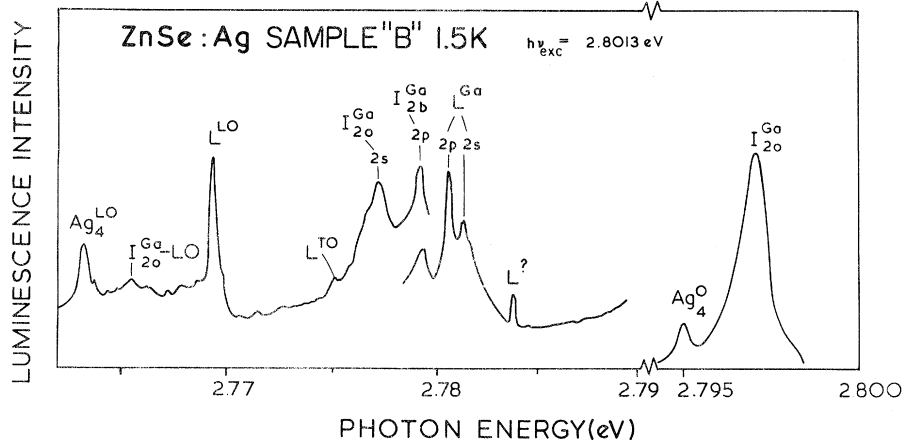


FIG. 2. Portions of the low-temperature photoluminescence of a ZnSe:Ag single crystal excited with tunable dye laser close to the fourth excited state d of the neutral donor BE. Components L^{Ga} represent the “two-electron” satellites of this particular DBE state, or donor electronic Raman scattering resonantly enhanced at the DBE, while “two-electron” satellites from lower lying DBE states, 0 and b , are also present as well as Raman scattering involving LO and TO phonons L^{LO} and L^{TO} . The principal DBE I_{20}^{Ga} and new Ag-related BE Ag_4^0 are shown on an expanded scale at the right. The much stronger coupling to LO phonons for Ag_4^0 is evident on the left. Component $L^?$ is an artifact of the spectrometer system.

energy of Ag_4^0 is closer to 2.7951 eV, but the relatively broad main DBE component I_{20}^{Ga} in Fig. 2 is downshifted by ~ 0.4 meV compared with expectation from the Ga donor in a dilutely doped, unstrained crystal.^{16,18} The identity of the dominant donor in this crystal is firmly established from the displacement energies of 20.7 and 19.9 meV observed for the “two-electron” DBE satellites labeled with superscripts $2p$ and $2s$ in Fig. 2, since these energies are close to the excitation energies $1s \rightarrow 2p$ and $1s \rightarrow 2s$ measured for the Ga donor.¹⁸ Components I_1^{Li} and Ag_3^0 , so strong for above-gap photoluminescence excitation (Fig. 1) are negligible for optical excitation close below E_{GX} , where there is a cluster of shallow DBE excited states. Despite the selective excitation of Ag_4^0 in this manner, such as I_{20}^{Ga} and its satellites, there is some considerable doubt as to whether Ag_4^0 also represents a DBE transition. The S parameter for LO coupling to this component is about 0.14, roughly 10 times larger than for the Ga donor (Table II). Such a large value of S_{LO} is more consistent with expectation for BE recombinations at some neutral center, as concluded for component I_0^a which appears just above the usual range of DBE transition energies for components I_{20} .¹⁶

We observed a further weak luminescence line Ag_2^0 near 2.7793 eV. This line also seems to relate to the presence of Ag, but is best seen under selec-

tive excitation just above E_{GX}^0 , near 2.809 eV. It may be the same as the highest energy of two luminescence components Ag_2^0 (2.7788 eV) and Ag_3^0 (2.7778 eV) reported by SG and very speculatively attributed to BE recombination at neutral acceptors, respectively, at an Ag-Na complex and at isolated Ag_{Zn} . These identifications must be regarded as tentative, especially since they depend partly upon use of a simple linear Haynes’s-rule relationship between the ABE localization energy E_{BX} and the acceptor binding energy E_A . This simple form of Haynes’s rule is known to be inappropriate for acceptors in ZnSe, just as it is for other direct-gap semiconductors.²⁰

The most striking BE luminescence in our Ag-doped ZnSe has a no-phonon line Ag_1^0 [Figs. 1 and 3(a)] called Ag_4^0 by SG. This spectrum contains relatively strong and richly structured sidebands due to phonon-assisted transitions (Table II). We have identified the broad wing at 2.745 eV with transitions of the Ag_1^0 BE assisted by the emission of ~ 2 -meV phonons. This interpretation contrasts with SG, who labeled this component Ag_3^0 and identified it with an independent ABE. The interpretation of SG is made very unlikely because we found the intensity ratio of these two luminescence components to be invariant between spectra from four independently grown layers of ZnSe:Ag. However, the most convincing proof for the pho-

TABLE II. Bound-exciton luminescence components in Ag- and Au-doped ZnSe (commonly present components of comparable type).

Component energy (eV)	Phonon (meV)	S factor	Identification
Ag ₄ ⁰ , 2.7951	LO(Γ) ^a	0.14	Neutral Ag associate
Ag ₃ ^{0b} , 2.7825	LO(Γ)	0.03	Neutral Ag ABE ^b (I ₁ ^{Ag}) ^b
Ag ₂ ⁰ , 2.7793			Unidentified Ag center
Ag ₁ ⁰ , 2.7470	LO(Γ)	~0.6	Neutral Ag _{Zn} -Ag _I associate or split interstitial
	2.0,2.7(L) ^c	~2	In-band resonances local modes
	1.6,2.4(A) ^c	~1.5	
	5.0 (L and A),7.7(A)		IBR overtone
	9.2,13.2,22.2(A)		Phonons
	26.3(L),26.4(A)		TO(Γ) phonon
Ag ₅ ⁰ , 2.664	LO(Γ)	~2	Neutral Ag _{Zn} -Ga _{Zn} associate ^b
I ₁ ^{Au} , 2.7900	LO(Γ)	0.05	Neutral Au ABE
(I ₁ ^{deep} , 2.7830)	LO(Γ)	0.32	Neutral Cu ABE ^b
(I ₁ ^{Li} or I ₁ ^{Li} , 2.7922)	LO(Γ)	0.05	Neutral Li ABE
(I ₁ ^{Na} or I ₁ ^{Na} , 2.7931)	LO(Γ)	0.03	Neutral Na ABE
I ₂ , ~2.7975	LO(Γ)	~0.01	Neutral DBE

^aLO(Γ) denotes long-wavelength longitudinal-optical lattice phonon.

^bHypothetical identification.

^cL denotes measurements from luminescence and A from absorption.

non satellite interpretation is obtained from a comparison of photoluminescence (PL) and PLE spectra in Fig. 3. Corresponding satellite structure appears (in the PLE spectrum) at an energy immediately *above* the line Ag₁⁰, which is the only common feature between the PL and PLE spectra, just as expected for a no-phonon transition. Thus, the Ag₅⁰ component of SG is actually a Stokes phonon

replica of Ag₁⁰, and involves two modes of energy close to 2 meV (Table II). This energy lies well within the continuum of acoustic phonons of the ZnSe lattice,²¹ which can be observed as a smooth satellite extending to a weak peak near 9.2 meV in the luminescence of certain other BE in ZnSe, such as the I₁^{deep} line near 2.782 eV.²

SG were led to the view that the broad com-

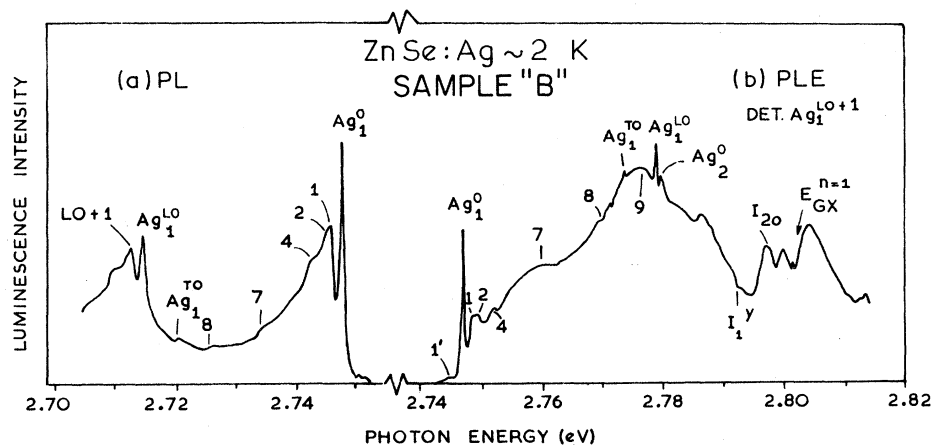


FIG. 3. (a) Low-temperature photoluminescence and (b) photoluminescence excitation spectra of a ZnSe:Ag single crystal recorded with a tunable dye laser. The no-phonon line Ag₁⁰ is the common feature between these spectra, while LO and TO phonon-assisted transitions appear in both spectra. The plain numbered structure is interpreted in terms of transitions involving the further phonons listed in Table II. Component 1 is apparently an anti-Stokes version of 1 arising because of small heating under the laser beam. Component Ag₂⁰ involves a different Ag-related BE than Ag₁⁰. The PLE spectrum contains dips at the strong absorption FE features E_{GX}ⁿ⁼¹ and E_{GX}ⁿ⁼².

ponents near 2.745 eV involved a separate BE by a misleading comparison with the Cd-O BE in GaP.²³ They observed that these components shifted 0.3 meV to higher energy when $^{107}\text{Ag} \rightarrow ^{109}\text{Ag}$ and interpreted this as a no-phonon isotope shift, like that observed for the Cd-O center when $^{16}\text{O} \rightarrow ^{18}\text{O}$. However, the correct comparison should be with the effects of Cd isotope substitution, since a significant upshift in the luminescence transition energy of a ~ 70 -meV phonon replica was observed when $^{114}\text{Cd} \rightarrow ^{110}\text{Cd}$ with no discernible shift in the no-phonon line, just the opposite of the effect of O isotope change.²³

In this example, the shift $\Delta\hbar\omega_R$ of the in-band resonant mode energy for an isotope mass increase $\Delta M=2$ in a mass of $M=107$ amu should be only $\sim +0.02_3$ meV according to the harmonic approximation

$$\Delta\hbar\omega_R = \frac{1}{2} \left[\frac{\Delta M}{M} \right] \hbar\omega_R. \quad (1)$$

Coupling to these low-frequency modes could be very anharmonic, so Eq. (1) consequently provides a large underestimate to $\Delta\hbar\omega_R$, although this equation fits very well for high-frequency modes in ZnSe. The SG estimate of $\Delta\hbar\omega_R$ may be too large by a factor of at least 2. Despite the quantitative disagreement which leads to a new interpretation, the qualitative isotope shift provides proof that this emission is due to Ag.

Low-energy modes related to heavy substitutional cations have been seen in GaAs (Ref. 24) and GaP (Ref. 25). The sharpness of the no-phonon line and the rapid decay (< 50 nsec) of the emission substantiate its BE nature.²⁶ Both properties are in striking contrast with those expected for dis-

tant donor-acceptor-pair (DAP) transitions²⁷ and observed in Sec. III B for other luminescence characteristic of ZnSe:Ag.

The general complexity and strength of the phonon coupling to the Ag_1^0 transition (Table II) compared with other BE in ZnSe such as I_1^{deep} suggests that a complex may be involved. (I_1^{deep} is a commonly observed BE in ZnSe, so called because it has a higher binding energy than other common BE's, and is thus deep.) The presence of *two* very-low-frequency modes (Table II) also suggests that the center may contain two Ag atoms according to arguments recently developed for Cu-related BE in GaP.²⁵ Given that the Ag_1^0 BE luminescence is very efficient, recent comparative studies on ABE in ZnTe (Ref. 28) suggest that the center is unlikely to be of the neutral ABE type, since Auger recombination is likely to form the dominant recombination channel for an ABE with E_{BX} as large as 55.3 meV. A second strong argument in disfavor of the neutral ABE model is provided by a comparison with the data on ZnSe:Ag (Sec. II C). There we see that the Au_{Zn} acceptor with significantly larger E_A than Ag_{Zn} (compare Tables II and III) may have an E_{BX} value only 13.0 meV, just 2.5 meV larger than for the shallow Li acceptor ($E_A = 114$ meV). The absence of an efficient luminescence in ZnSe:Ag of comparable spectral form to Fig. 3 is inconsistent with the attribution of the Ag_1^0 Be to ABE recombinations at the isolated substitutional noble-metal acceptors. However, the general behavior we describe is perfectly consistent with an assignment to BE recombination at a *neutral* associate such as the $\text{Ag}_{\text{Zn}}\text{-Ag}_I$ pair. The corresponding center for ZnSe:Ag might be hard to prepare given the large ionic radius of

TABLE III. Binding energies of the lowest acceptor states from DAP PLE, ABE, and acceptor electron Raman scattering (meV).

Crystal and acceptor	E_A	E_{2s}	E_{3s}	E_{4s}	$E_{2p_{5/2}(\Gamma_8)}$	$E_{2p_{5/2}(\Gamma_7)}$
ZnTe:Cu ^a	148	22.4	10.5	6.1	16.3	13.1
ZnTe:Ag ^b	123	20.7	10.0	5.7		
ZnTe:Au ^c	272	28.9	13.8	8.4	16.3	12.6
ZnSe:Li ^d	114	31.3	16.2	11.5	28.2	21.0
ZnSe:Na ^d	128	30.4	17.5	13.3	27.6	21.2
ZnSe:Ag	431	37.5 ^e	18.5 ^e	11.7		

^aReference 8.

^bReferences 9 and 10.

^cReference 37.

^dReference 63.

^eUsed in fitting to the $n^{-1.76}$ law.

Au^{1+} (1.37 Å) compared with Ag^{1+} (1.26 Å). The repulsive energy due to local lattice distortion could easily outweigh the electronic component of the pair bond for $\text{Au}_{\text{Zn}}-\text{Au}_I$. It seems likely that the Ag_1^0 center could have a split-interstitial configuration, as observed for generically similar complexes in Si (Ref. 29) and GaP (Ref. 25).

The identifications of the other phonons observed in the Ag_1^0 BE spectrum are suggested in Table II. Comparison of the PL and PLE spectra confirms the identity of the component Ag_1^{LO} despite the closeness of its energy, 2.7787 eV to component Ag_3^0 of SG. It is most unlikely that a component Ag_1^{TO} whose displacement energy is consistent with the long-wavelength transverse-optical (TO) phonon of the ZnSe lattice would appear in both the PL and PLE spectrum if at least most of the Ag_1^{LO} component was not to be interpreted in terms of coupling to LO phonons. The coupling strength to the long-wavelength LO phonon is generally stronger than to TO in such spectra for a polar lattice, due to the macroscopic electric field of the LO phonons. Comparison of the PL and PLE spectra also suggests that component Ag_2^0 in Fig. 3 is not due to a 32.8-meV true local mode, an unlikely possibility in any case since $M_{\text{Ag}} \gg M_{\text{Zn}}$. It is possible that Ag_2^0 is caused by a BE involving an independent center, since we have already mentioned that a weak luminescence line appears at a similar energy (2.7793 eV) in the same crystal. This component must then appear in the PLE spectrum of the Ag_1^0 PL as a result of inter-site BE tunneling before radiative recombination, occurring despite the relatively large BE localization energy of $E_{\text{BX}} \sim 22.5$ meV for Ag_2^0 . It seems unlikely that Ag_2^0 could be an excited electronic state of the center responsible for Ag_1^0 , both because no luminescence from Ag_2^0 should then occur at 2 K and because the intensity ratio Ag_2^0 to Ag_1^0 was significantly variable between samples. A 32.8-meV electronic splitting *could* arise in various ways for an exciton bound to an axial associate such as $\text{Ag}_{\text{Zn}}-\text{Ag}_I$.^{20,25} However, the electron-hole exchange splitting ΔE is likely to be small for this BE as a consequence of the low electron-to-hole mass ratio in ZnSe, rather like the Bi BE in InP,²⁹ which also binds the hole by short-range forces. In addition, the axial stress cannot split the conduction band in ZnSe and produce an attractive local potential for electrons as well as holes and hence a large value of ΔE , as seems to occur for Cu-related associates in GaP.²⁵

The neutral $\text{Ag}_{\text{Zn}}-\text{Ag}_I$ is expected to form a BE state through strong interaction with the *hole* be-

cause of the residual effect of the large central-cell enhancement of the binding energy of the isolated Ag_{Zn} acceptor (Sec. III B). The reduction in total electron-hole binding energy from ~ 460 meV of the distant DAP to ~ 73 meV at the associate could occur very readily as a consequence of the influence of the interstitial donor on the Ag_{Zn} acceptor,²⁷ as can be seen from Eq. (3) below with $R \rightarrow R_{\text{associate}}$.

Evidence for DAP associates involving Ag_{Zn} has been obtained from local vibration mode (LVM) studies on ZnSe:Cu, ZnSe:Ag, and ZnSe:Au co-doped with Al donors.³⁰ Strong preferential pairing is necessary for such centers to be detected by this technique. The argument raised above that associates will not form for ZnSe:Au is inapplicable for these associates, since the number of LVM observed and their relative energies suggests that the pair is $\text{Au}_{\text{Zn}}-\text{Al}_{\text{Zn}}$. The ionic radius of Al^{3+} (0.50 Å) is significantly less than Zn^{2+} (0.74 Å), so that the local strain field in this associate tends to compensate for the effect of the larger Au ion and enhance the pairing promoted by the valency differences and core potential effects. Unfortunately, associates such as $\text{Ag}_{\text{Zn}}-\text{Ag}_I$ are not suitable for detection by LVM spectroscopy according to the phonon properties in Table II. On the other hand, many of the luminescence properties described above could be accounted for by an $\text{Ag}_{\text{Zn}}-\text{Al}_{\text{Zn}}$ associate. However, there is no evidence in our spectra of the ~ 45 -meV local modes expected for an associate containing Al_{Zn} (Ref. 31) (Fig. 3). We also cannot so readily account for the presence of *two* in-band-resonance low-frequency modes with a center containing only one Ag_{Zn} atom. In addition, we have no explanation on the $M_{\text{Zn}}-\text{Al}_{\text{Zn}}$ associate model for the absence from ZnSe:Au of BE luminescence comparable to Ag_1^0 . Since our crystals were heavily doped with Ag, we conclude that luminescence from any pairing of Ag_{Zn} with residual Al donors which may be present is likely to be negligible in comparison with that of the $\text{Ag}_{\text{Zn}}-\text{Ag}_I$ associate. We have already noted that Al_{Zn} is not the major donor species in these particular liquid-phase epitaxial (LPE) ZnSe crystals. Any BE luminescence from $M_{\text{Zn}}-\text{D}_{\text{Zn}}$ associates should fall at an appreciably lower transition energy compared with $M_{\text{Zn}}-M_I$, as a general consequence of the larger interion separation for the cation sublattice center.²⁷ A further Ag-related BE luminescence which may involve such an associate is mentioned below. It is also possible that the poorly resolved and relatively weak component on the high-energy wing of the distant DAP

luminescence of ZnSe:Ag described in Sec. III C may result from such associates, this luminescence then being unmasked by Au_{Zn} - Au_I contributions for reasons already cited. The very strong phonon-coupling characteristic of the Au_{Zn} acceptor makes resolution of these spectral contributions very difficult. However, luminescence from the high-energy possible-BE-associate component does appear to be favored at intermediate temperatures, as expected (Fig. 13 below).

Besides the positive features associated with phonon-assisted absorption processes already discussed (Table I), the PLE spectrum of the Ag_1^0 BE luminescence (Fig. 3) contains a maximum at the DBE component I_{20} , presumably due to tunneling energy transfer from this very diffuse BE state. The pronounced minimum near E_{GX} is a common feature of PLE spectra, caused by enhanced surface recombination for the strongly absorbed light near this energy.

The form of the PLE spectrum in Fig. 3 was invariant for detection at Ag_1^0 -LO and Ag_1^0 -2LO, except for a decrease in the contribution of Ag_2^0 in the latter case, but the structure was significantly less pronounced for luminescence detection at Ag_1^0 -3LO. This is caused by the contribution of luminescence from a system with no-phonon line Ag_5 near 2.664 eV (Table II) not readily observed for above-gap excitation (Fig. 1). This spectrum was not studied in detail since it was weak. It exhibits strong, complex, but not very clearly defined phonon coupling because of overlap with the Ag_1^0 phonon structure. It is possible that this spectrum may represent BE recombination at Ag_{Zn} - Ga_{Zn} associates, since a decrease in transition energy of 83 meV relative to Ag_1^0 might result from the necessary increase in separation between the donorlike and acceptorlike members of these associates.²⁷

The temperature dependence of the Ag_1^0 BE luminescence is shown in Fig. 4, recorded under cathodoluminescence (CL) excitation for a crystal showing relatively weak shallow DAP luminescence. Above the lowest temperatures, ≥ 20 K, the near-gap luminescence becomes dominated by FE luminescence. The Ag_1^0 spectral features broaden and the luminescence intensity becomes rapidly weaker than the FE luminescence above ~ 60 K. The total intensity I_T follows the usual Arrhenius relationship above ~ 65 K:

$$I_T/I_0 \propto \exp(-\epsilon_A/kT). \quad (2)$$

The thermal activation energy ϵ_A derived from Eq. (2), which applied to measurements between

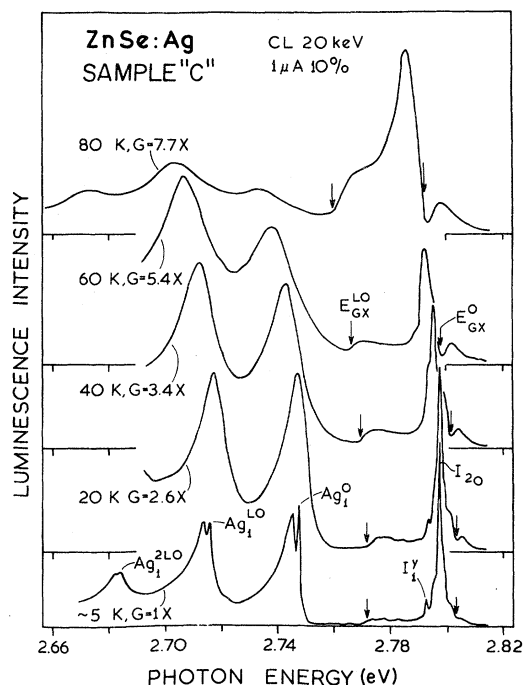


FIG. 4. Temperature dependence of the near-gap cathodoluminescence of an Ag-doped ZnSe single crystal selected to have negligible shallow DAP luminescence, to facilitate measurement of the thermal quenching of the Ag_1^0 -related Ag BE luminescence. Notation as in Fig. 1. The vertical arrows denote the FE energy E_{GX}^0 and the threshold energy for LO(Γ) phonon-assisted FE recombination for zero FE kinetic energy. These energies decrease as E_G decreases with increasing T , non-linearly at these low temperatures. The relative ordinate recording gain is denoted by G .

~ 65 and ~ 120 K, was $\sim 50 \pm 3$ meV. This is close to both the value of $E_{BX} = 55$ meV for Ag_1^0 , and also to the value of the hole binding energy at the associate, about 50 meV. The latter value is estimated from the usual approximation for an associate which is expected to bind one electronic particle much more tightly than the other,³² here the hole. On this model, the contribution of the electron to the total electron plus hole binding energy of 73 meV should be slightly less than the effective-mass binding energy of a donor, about 26 meV in ZnSe.¹⁶ It is more plausible to suggest that the value of E_A measured above 65 K represents the hole ionization energy. The agreement with experiment provides useful support for the model of unequal binding energies, which is a natural consequence of the model we have proposed for the Ag_1^0 BE.

B. Donor-acceptor-pair luminescence of Ag-doped ZnSe

The green luminescence which dominated the visual impression is contained in a relatively broad spectrum with Huang-Rhys coupling factor $S \sim 4$ and poorly resolved phonon sidebands partly due to coupling to a wide range of phonons of the ZnSe lattice, not only to the long-wavelength LO phonon (Fig. 5). The LO(Γ) phonon remains significant for the structure at the high-energy limit of the DAP spectrum, discussed further below, but the average periodicity near the overall peak of the envelope is close to 26 meV, of the order of the

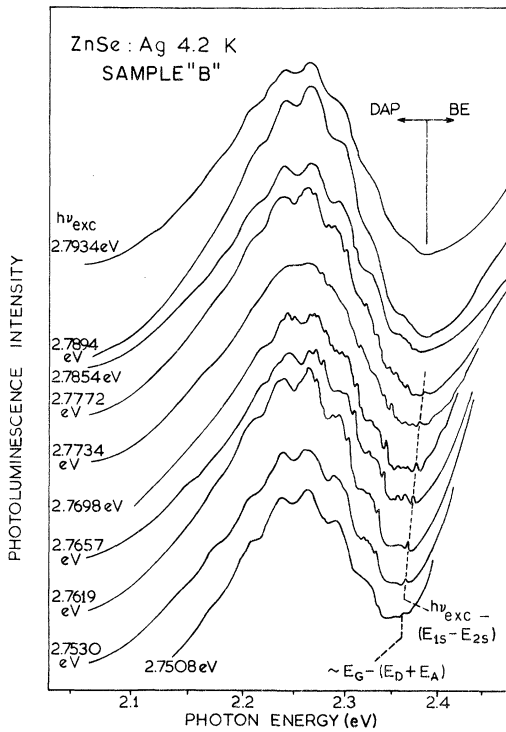


FIG. 5. Variation of the broad green low-temperature photoluminescence band characteristic of ZnSe:Ag with the energy $h\nu_{\text{exc}}$ of the excitation from a tunable dye laser. The overall weak intensity modulation seen most clearly in the bottom and top spectra is caused by prominent coupling to optical phonons, repeating the no-LO phonon structure near 2.37 eV. The considerable additional structure in this region for intermediate values of $h\nu_{\text{exc}}$ is due to selective excitation of luminescence from donor-acceptor pairs (DAP) within a particular narrow range of DAP separation, involving excitation to several different excited states of the deep Ag acceptor and their acoustic phonon replicas. The principal acceptor excited state involved is $2s$. Selective excitation is only possible when $h\nu_{\text{exc}} - (E_{1s} - E_{2s})$ is larger than $E_G - (E_D + E_A)$.

TO(Γ) energy (Fig. 3) rather than 32 meV. However, this energy is likely to be selected as being close to the maximum of the density of states of optical phonons⁶² rather than there being any particular significance in the coupling to TO(Γ) phonons, which is not strong in these types of optical spectra (Figs. 1 and 3). The spectral envelope remains unaltered for all excitation energies $h\nu_{\text{exc}} > 2.7894$ eV. Under these conditions, the weak no-phonon luminescence is contained in a broad band centered near 2.365 eV, typically diffuse because of the wide range of DAP separations R which contribute to the luminescence according to the well-known relationship²⁶

$$h\nu = E_G - (E_D + E_A) + e^2/\epsilon R. \quad (3)$$

However, strong proof that this peak is a DAP transition is obtained from the spectral details which emerge as the energy of the exciting dye laser is tuned below 2.7894 eV. Quite sharp components appear near the high-energy limit of the green luminescence band, together with a few well-defined phonon replicas, all superimposed upon the broad structure which also tends to become slightly better defined. These components appear in turn as the laser energy is reduced, and die away to be replaced by others until the spectrum becomes free of sharp structure for $h\nu_{\text{exc}}$ below 2.751 eV.

This type of behavior is characteristic of selective excitation of photoluminescence³² (SPL) within the quasicontinuous distribution of DAP excitation energies which extend from E_G down to $E_G - (E_D + E_A)$ according to Eq. (3). Given sufficiently large values of R , the internal excitation energies of the acceptor E_A are insignificantly perturbed by the interaction with the distant donor.³³ The inset of Fig. 6 shows that an excitation event which creates a hole in an excited state of the acceptor and places an electron in the ground state of a distant donor can also give rise to the same well-defined luminescence energy after recombination within the selected DAP. This process can be observed either in PLE spectra, resulting in the sharp positive line Ag_{2s}^0 in Fig. 6(b), or in SPL spectra as shown in Figs. 6(a) and 5. The latter SPL technique has the advantage that the structure does not become obscured by the BE and FE, which generally produce strong minima in DAP PLE spectra^{32,34} as observed here [Fig. 6(b)]. The energy difference between the spectrometer setting and the laser energy corresponds to an internal energy within the donor or acceptor in both SPL and

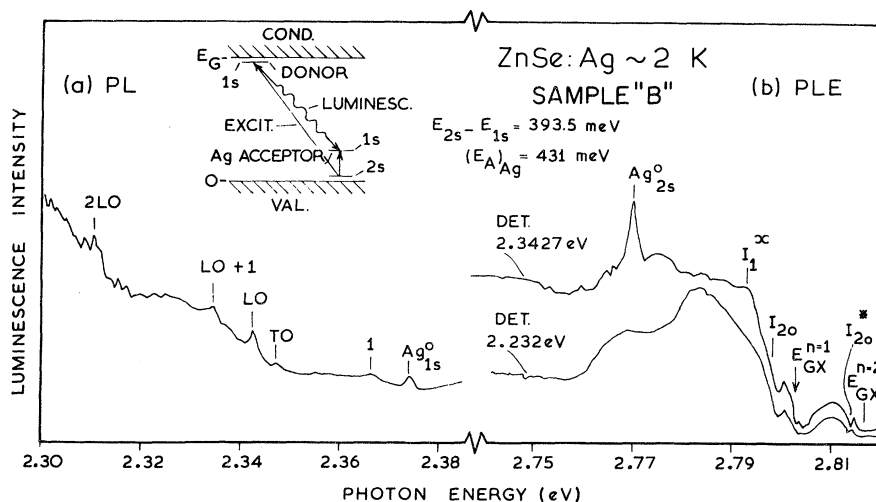


FIG. 6. Comparison of (a) the low-temperature selectively excited photoluminescence and (b) photoluminescence excitation spectra for the green DAP luminescence of ZnSe:Ag. The SPL spectrum in (a) was selected for an intermediate value of $h\nu_{\text{exc}}$ in Fig. 5, to emphasize the sharp structure. The PLE spectra in (b) are compared for the indicated values of $h\nu_{\text{det}}$ which provide maximum contrast between contributions of selectively (upper) and nonselectively excited DAP luminescence. The broad thresholds in the latter near 2.760 and 2.774 eV are discussed in the text. Notation is as Fig. 1 except that I_{20}^* represents a neutral DBE derived from the $n=2$ FE $E_{GX}^{n=2}$. The mechanisms of selective DAP excitation are indicated in the inset.

PLE spectra, as is clear from the inset of Fig. 6. We provide below evidence for the attribution of this excitation process to the acceptor, rather than to the donor.

The PLE spectrum in Fig. 6(b) for detection at 2.232 eV, near the peak of the green luminescence spectrum (Fig. 5) contains no sharp positive structure, but only broad thresholds near 2.760 and ~ 2.774 eV, respectively, ~ 62 and ~ 48 meV below E_G taken to be 2.822 eV.¹⁶ The general form of the PLE spectrum for the nonselectively detected Ag DAP luminescence can be better appreciated by the data in Fig. 7 taken with the W lamp, monochromator, and filter combination, in this case with a Wratten W47 filter before the sample and a combination of two W21 and one W61 filters after the sample and before the S20 response photomultiplier detector. The broad phonon-assisted absorption of the DAP system was too weak to be detected below ~ 2.45 eV, so the weak overlap between the PL and PLE spectra near 2.38 eV expected from Fig. 5 could not be confirmed. However, much of the rise near 2.55 eV is due to this process, and the overall shape is better established from this corrected PLE spectrum than from the uncorrected dye-laser spectrum in Fig. 6. The expected low-energy threshold for nonselective excitation of DAP PL is at $E_G - (E_A)_{\text{Ag}}$, or ~ 2.39 eV according to Table III.

The observed threshold near 2.46 eV in Fig. 7 falls near the 2LO phonon replica of this threshold, which corresponds to the region of steepest rise in the PL spectrum. The broad thresholds near 2.76 and 2.774 eV are quite apparent in Fig. 7, as in Fig. 6, but the detailed near-gap structure is not clear apart from the dip near E_{GX} .

If much shallower hole traps than $(E_A)_{\text{Li}} = 114$ meV exist to account for the broad thresholds in Figs. 6 and 7, they can promote green Ag DAP luminescence by a two-step process. For example, one photon of energy near 2.77 eV may photoneutralize a compensated Ag acceptor through exciting an electron to the conduction band, while a second promotes a similar transition from the 62- and 48-meV hole traps, so releasing extra electrons. Some of these extra electrons may be trapped at shallow donors to produce green Ag distant DAP luminescence. It is possible that the ~ 48 -meV hole trap may be the neutral Ag associate responsible for the Ag_1^0 BE according to the energies discussed in Sec. III A. An alternative scheme may be considered, in which the ~ 62 - and ~ 48 -meV traps are attributed to electron states. A corresponding sequence of events can be devised to explain the occurrence of the associated absorption edges in the PLE spectrum. However, this scheme seems less attractive, both because it is rather more difficult to obtain such moderately deep electron

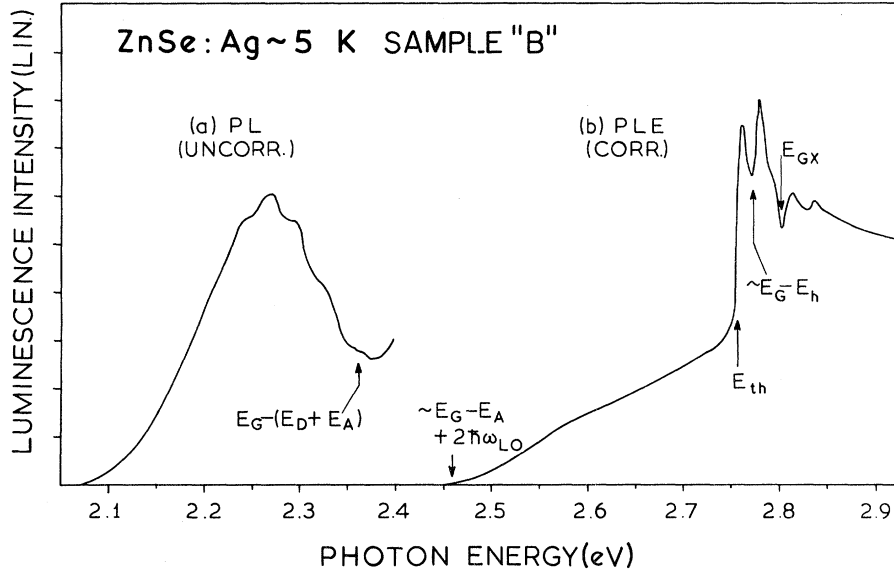


FIG. 7. (a) Low-temperature PL and (b) PLE spectra from an Ag-doped ZnSe single crystal involving the green distant DAP luminescence. The PL was excited by ~ 50 -mW 360-nm light. A lamp and monochromator combination was used for the PLE, with a filter combination before the detector which transmitted PL between ~ 2.18 with ~ 2.28 eV. Various energies involving the deep Ag acceptor E_A are noted, together with the PLE thresholds E_{th} near 2.76 eV and at $E_G - E_h$ near 2.774 eV noted in Fig. 6. E_h is the approximate binding energy of a hole at the center responsible for the Ag_1^0 BE. The FE energy E_{GX} is again marked by a dip.

traps in ZnSe and because no additional DAP bands involving either the Ag or Li acceptors are seen.

The high-energy region of the green Ag DAP SPL spectrum contains structure which can be interpreted in terms of three no-phonon transitions labeled $h\nu_{exc} - (E_{1s} \rightarrow E_{ns})$ in Fig. 8, where $2 < n < 4$, together with an acoustic phonon replica of energy $h\omega_{AC} \sim 8.4$ meV and the LO phonon of energy ~ 32.0 meV. The assignments are made by comparison with similar spectra in ZnSe (Ref. 12) and ZnTe (Ref. 34), where it has been found that absorption processes into s -like acceptor excited states predominate even though transitions to p -like states can also be observed as a result of the breakdown of T_d symmetry due to the presence of the distant donor. The phonon replicas can be distinguished by their constant intensities relative to the no-phonon components, while the intensities of the latter grow and fade as the appropriate displacement energy moves into and out of the most favorable position for selective excitation of distant DAP through the different acceptor excited states.³³ It is a problem to derive the best estimate of the acceptor ionization energy E_A from the $1s \rightarrow ns$ excitation energies provided from these spectra, since the energies of excited as well as

ground s states are subject to significant central cell enhancements. Comparison with the excited states of the deepest acceptors seen so far in ZnTe (Refs. 8 and 35) and the shallow acceptors Li and Na in ZnSe (Ref. 12) shows that the energies of the excited s -like states can be described by a semi-empirical law

$$E_{ns} = E_0 n^{-m}, \quad (4)$$

where E_0 is a hypothetical energy for a $1s$ state, in all cases much shallower than actually observed, and m is a constant close to 1.76 for several acceptor spectra in ZnTe (Ref. 36) and in GaP (Ref. 32). Assuming this law holds for the deep Ag acceptor in ZnSe, as is approximately true for the shallow acceptors,⁶³ the observed displacement energies $E_{1s} \rightarrow E_{ns}$, $2 < n < 4$ yields $(E_A)_{Ag} = 431 \pm 2$ meV. The derived excited-state energies are compared with those of several other acceptors in Table III. The close similarity of the excited states resolved in Fig. 8 with those of other acceptors, together with the magnitudes of the excitation energies in Table III makes it quite certain that the structure is due to an acceptor, since the energies and patterns of excited states of donors in ZnSe are quite different.¹⁶

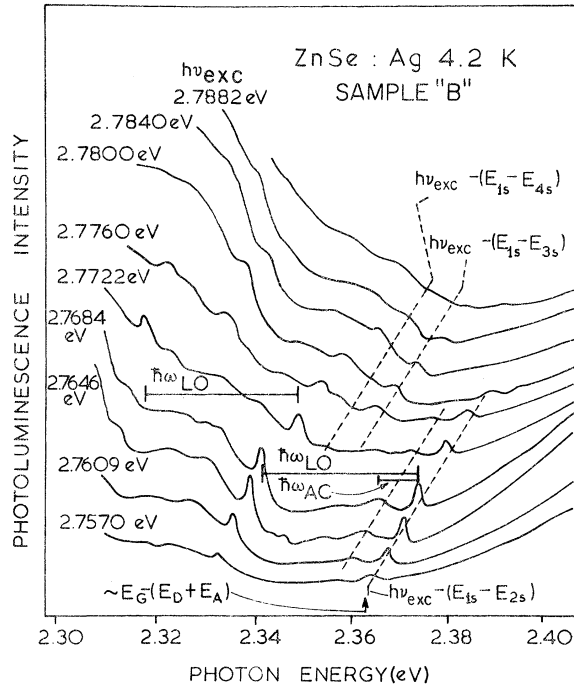


FIG. 8. Detail of the high-energy portion of the low-temperature, selectively excited green DAP photoluminescence of ZnSe:Ag for the indicated values of excitation by a tunable dye laser, $h\nu_{exc}$. Identification of the structure in terms of no-phonon transitions involving the indicated excited states of the deep Ag_{Zn} acceptor and acoustic (AC) or optical (LO) phonon replicas is possible from the evolution of the spectra with $h\nu_{exc}$. Comments on the SPL process are as in Fig. 5.

An independent check upon this value of E_A can be obtained from the positions of $E_G - (E_D + E_A)$ estimated in Figs. 5 and 7 from the positions of the no-phonon line when the selective excitation process involving the $1s \rightarrow 2s$ acceptor excitation just fades.³² Since $E_G = 2.822$ eV,¹⁶ and the minimum value of $E_G - (E_D + E_A)$ is 2.360 eV [Fig. 7, with maximum allowance for the residual value of $e^2/\epsilon R$ in Eq. (3)], then $(E_D + E_A) = 462$ meV. Assuming $E_D = 27.2$ meV for the dominant Ga donor in this crystal (Sec. III A), we derive $E_A = \lesssim 435$ meV, consistent with the estimate from Table III. Previous estimates for $(E_A)_{Ag}$ in ZnSe were obtained from photoconductivity excitation spectra³⁷ or from the peak energies of broad luminescence bands³⁸ with inappropriate corrections for the influence of phonon coupling. These much less precise techniques produced considerable overestimates of $(E_A)_{Ag}$, close to 0.6 eV.

It is of considerable general interest that these spectra for the deep Ag acceptor in ZnSe represent by far the deepest center for which the DAP SPL

process has been used to derive detailed estimates of E_A . The next deepest is the Au acceptor in ZnTe (Table III). However, in this case, the best information was obtained from the "two-hole" satellites of the Au neutral ABE luminescence line,³⁶ a technique which reveals similar displacement energies.¹⁰ We have not been able to observe "two-hole" satellites under excitation in the 2.747-eV Ag_1^0 BE, which supports the conclusion in Sec. III A that this does not involve the isolated Ag neutral ABE. However, we have not seen such replicas from the Ag_3^0 BE in Figs. 1 and 2. It is not clear whether this is because these replicas are very weak and easily lost against the strong luminescence of other types excited by light in this energy region or because the identification of Ag_3^0 suggested in Sec. III A is incorrect. If the latter holds, we would have to conclude that the Ag ABE has not been detected. Although this is possible due to the Auger process which may be important for BE of large E_{BX} ,²⁸ the attractive sequence of ABE for Cu, Ag, and Au described in Sec. III C would no longer be followed. A reason for the weakness of "two-hole" satellites for acceptors of this class, involving atoms with a tendency to an "open-shell" inner configuration, follows from the discussion in Sec. I. The influence of the open d shell on the acceptor ground state when this becomes much deeper than in ZnTe may seriously reduce the overlap with the effective-mass-like excited states to which the ground state must connect in the "two-hole" process.²⁰

Further evidence for the assignment of the green Ag luminescence to distant DAP recombinations comes from two sources. First, the low-temperature time decay of this luminescence is relatively slow and nonexponential at all decay times (Fig. 9), a hallmark of interimpurity recombination over large distances.²⁷ Second, the Arrhenius plot of the integrated intensity according to Eq. (2) gives a thermal activation factor $\epsilon_A = 400$ meV above ~ 330 K (Fig. 10) agreeably close to our estimate of $(E_A)_{Ag}$. The spectrum broadens with increasing temperature, particularly on the high-energy wing, as expected, and shifts progressively to lower energy above ~ 50 K as the band-gap reduction outweighs the effect of thermal broadening (Fig. 11).

C. Bound exciton luminescence of Au-doped ZnSe

The near-gap luminescence of two Au-doped ZnSe crystals both showed the new I , shown as the

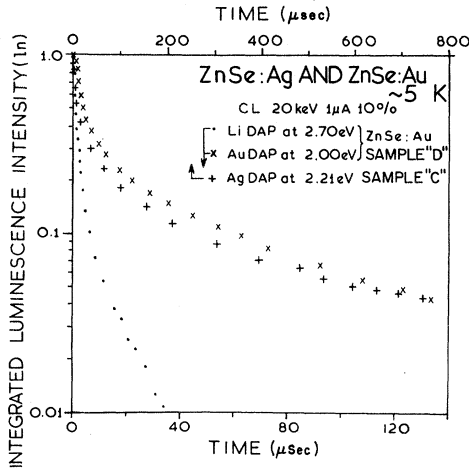


FIG. 9. Time decay of the low-temperature distant DAP luminescence involving the shallow acceptor Li (lower abscissa scale) and the deeper acceptors Ag (upper abscissa scale) and Au (lower abscissa scale). The luminescence was detected within an energy interval of a few meV at the overall peak intensity of each DAP spectrum near the indicated photon energies.

line labeled I_1^{Au} in Fig. 12. Energy downshifts of ~ 1 meV caused by inadvertently-present strain, possibly influenced by the doping of the epitaxial region with the large-radius Au atoms, were recognized from well-established BE such as I_1^{deep} or I_1^x . This was possible also for the DBE, once the identity of the dominant donor was determined from the "two-electron" satellites observed with resonant excitation. The energies of the components shown in Table II have been corrected for these shifts. It is quite clear that a new BE is introduced to a degree which increases with the Au concentration and is ~ 2.4 meV deeper than I_1^x , corresponding to $E_{BX} \sim 13.0$ meV. The Huang-Rhys factor for this new line is 0.05, less than for Li but more than for Ag or Na. The dominant donor for the crystal in Fig. 12 was Cl, but the second less heavily Au-doped crystal showed dominant Ga donors. Both crystals exhibited Li BE and DAP spectra. No other significant new BE lines were observed from either of these crystals. We have already discussed in Sec. IIIA the probable reason why there is no analog of the Ag_1^0 BE for ZnSe:Ag.

Our tentative interpretation that the Au ~ 2.790 -eV A_1^{Au} BE line is caused by neutral ABE recombinations at the deep Au acceptor is a consequence of there being no other candidate, together with the place of this ABE in the sequence $Li \rightarrow Ag \rightarrow Au \rightarrow Cu$ for ZnSe (Tables I and II). Clearly, the variation of E_{BX} with E_A is very weak

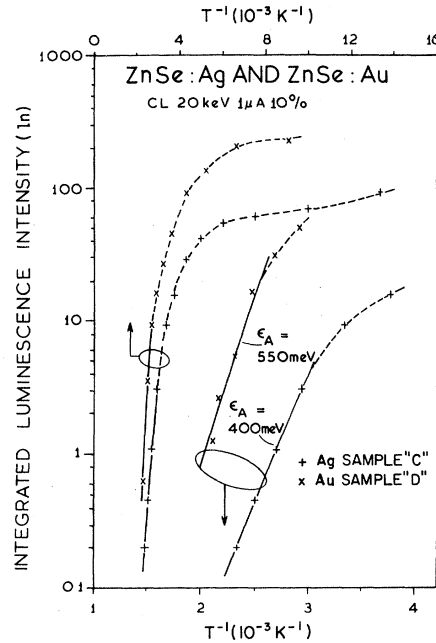


FIG. 10. Variation with sample temperature of the integrated luminescence intensity of the broad green and red PL bands, respectively attributed to distant DAP recombinations involving the deep Ag and Au acceptors. The upper pair of curves refer to the $10^3/T$ K^{-1} scale at the top, while the lower pair refer to the lower, expanded abscissa and yield the indicated thermal activation energies from their high-temperature slopes. The upper curve for the Ag-doped crystal yields an activation energy of about 20 meV in the low-temperature portion (below ~ 150 K), which probably represents thermal ionization of the shallow donor.

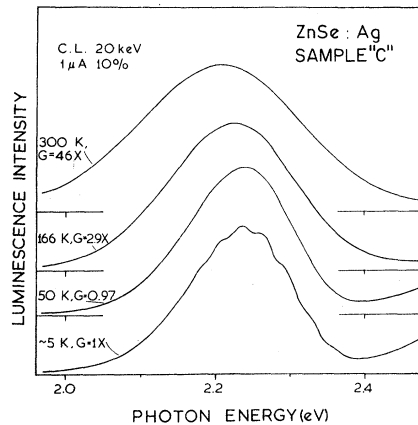


FIG. 11. Characteristic green luminescence band of ZnSe:Ag measured at the different temperatures under the indicated conditions of electron-beam excitation. The relative ordinate recording gain is denoted by G . The rapid loss of spectral structure caused by the strong phonon coupling obscures the change in dominant recombination mechanism from distant DAP at 5 K to free electron at neutral acceptor at ≥ 50 K.

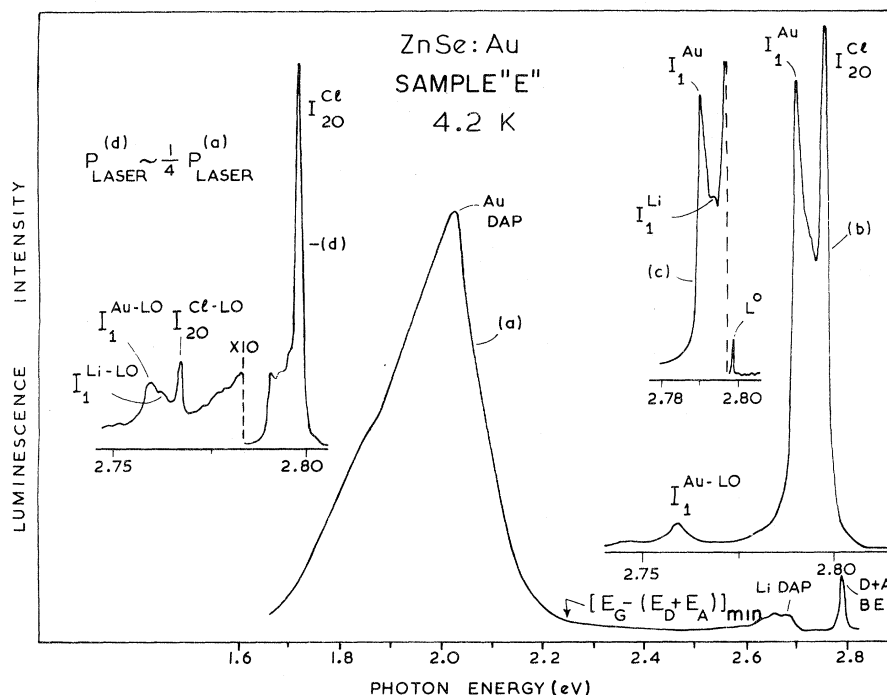


FIG. 12. Low-temperature photoluminescence from a single crystal of ZnSe: Au. Spectrum (a) shows the broad red luminescence characteristic of Au doping, distorted near 2.02 eV by the spectrometer response (compare with Fig. 13), together with relatively weak blue distant DAP luminescence introduced by the shallow Li acceptor and weak blue BE. Spectrum (b), recorded for excitation above E_G , and spectrum (c), recorded for excitation near the dominant neutral DBE due to Cl donors, show details of the shallow BE. These include a weak shoulder from the Li neutral ABE and a much stronger contribution from a new ABE attributed to the deep Au acceptor. Spectrum (d) shows that the intensity ratios $(I_1^{\text{Au}} + I_1^{\text{Li}})/I_{20}^{\text{Cl}}$ and $I_1^{\text{Au}}/I_1^{\text{Li}}$ decrease with decrease in excitation intensity and also that both I_1 lines have much stronger LO phonon coupling than I_{20}^{Cl} .

and nonlinear. Essentially no change in E_{BX} occurs from $E_A = 114$ (Li) \rightarrow 431 (Ag) meV, while further increase to $E_A = 650$ meV results in an increase in E_{BX} by ~ 9 meV, to almost double (E_{BX}). Although this type of behavior is well established²⁰ for acceptors in other direct-gap semiconductors such as GaAs, InP, and ZnTe, the insensitivity of E_{BX} to increases in E_A is demonstrated here to remarkably large values of E_A . It is most likely that this is caused by the character of these deep hole traps being more atomiclike than in ZnTe. This in turn is largely a consequence of the decrease in energy of the valence-band states dominated by the more electronegative Se anion relative to the energies of the transition-metal (TM) substituents. This causes a considerable decrease in the TM-host differential electron affinity for the whole range of TM species when the Te anion is replaced by Se (Sec. I). It has been argued that a strong admixture of d -like character which results from this change may remove the possibility of binding an exciton to a neutral TM "acceptor,"³⁹ although this can never be so for acceptors formed from

main-group impurity substituents.²⁰ No conventional neutral ABE has been observed for Cu_{Zn} in ZnS and particularly ZnO where the TM has essentially pure $\text{Cu}^{2+} 3d^9$ ground-state character. We have seen in Sec. I that ZnSe lies in the difficult transitional region between this extreme and ZnTe, where these TM introduce quasi-effective-mass-like acceptor states with strongly optically active, essentially conventional neutral ABE. That is, ZnSe falls close to the center of Fig. 1 of Robbins and Dean.¹¹

The enhanced contribution of d atomic character for ZnSe compared with ZnTe can qualitatively account not only for the abnormal insensitivity of E_{BX} to E_A but also for the relatively weak LO phonon coupling. The latter property relates directly to the small range of E_{BX} and also to the fact that coupling to long-wavelength lattice LO phonons is not a significant general feature of "conventional" TM spectra because of the very weak overlap between the $3d$ core states and the bonding states made up from the anion ligands. This mixture of atomic and ligand character in the

bound hole wave function also produces peculiar magneto-optical properties to be described for the TM Cu elsewhere.

D. Donor-acceptor-pair luminescence of Au-doped ZnSe

The most striking visual feature of Au-doped ZnSe is the introduction of red luminescence. The spectral form of the broad band responsible for this effect is distorted in Fig. 12, due to an anomaly in the detector response near the peak at ~ 2.02 eV. The correct form is closer to the bell-shaped curve characteristic of strong phonon coupling shown in Fig. 13, which also exhibits the temperature dependence of the spectra, including the great decrease in the relative intensities of the near-gap components between 5 and 300 K. The form of the time decay of the red luminescence was rather similar to that of the Ag green DAP luminescence (Fig. 9). The difference in time scale is probably a consequence of a difference in the donor doping levels between the two crystals, since a comparison of the DBE components in Figs. 2 and 12 suggests that the Au-doped crystals are more heavily doped.

The much slower decay rate for the Au luminescence compared with the Li DAP luminescence for the same crystal (Fig. 9) indicates that the spread of the wave function of the much shallower Li acceptor contributes significantly to the electron-hole wave-function overlap for this DAP.²⁷ The relatively slow and strongly nonexponential form of the time decay of the red Au luminescence once again strongly suggests recombinations within a wide distribution of DAP separations.

Because of the significant increase in the strength of phonon coupling between the Ag- and Au-related spectra, we can see no trace of residual structure from discrete phonons or of no-phonon transitions. Thus, the selective-excitation technique used in Fig. 8 to establish the value of $(E_A)_{Ag}$ cannot be applied to Au. This effect is by itself sufficient to remove the possibility of using the ABE to establish E_A from "two-hole" satellites, since the phonon coupling in these spectra should be very similar to that in the DAP spectra. Indeed, we were again unable to recognize such satellites even for selective excitation into I_1^{Au} , just as we could not for the I_1^{deep} line believed to be the ABE of the deep Cu acceptor. However, the trend in properties suggested from a comparison of the

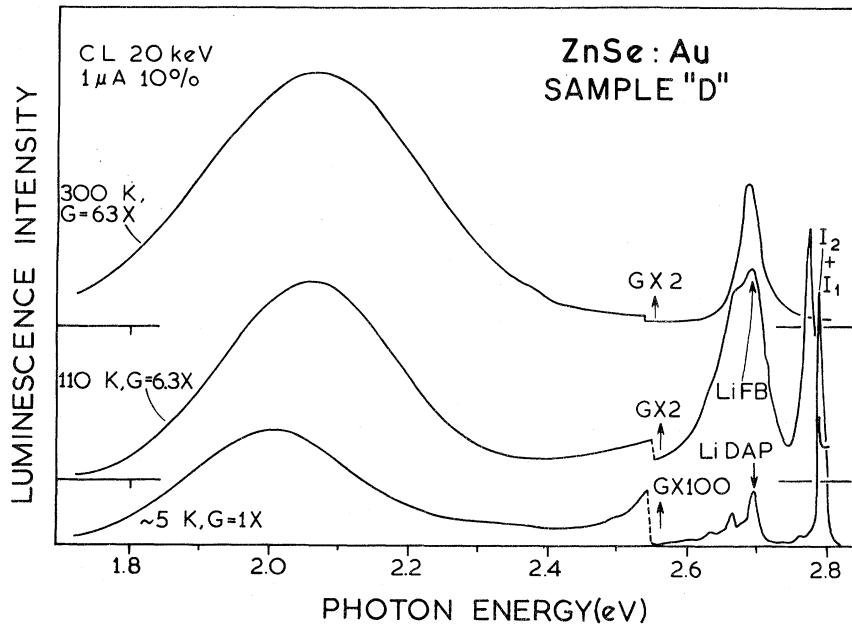


FIG. 13. Overall visible luminescence of ZnTe:Au recorded under the indicated conditions of electron-beam excitation and temperature for a crystal more lightly Au-doped than in Fig. 12. The relative ordinate recording gain G at left refers to the near-gap spectral region on right. Further changes of gain were necessary to display the broad red band attributed to distant DAP recombinations involving the deep Au acceptor at $T < 50$ K. It is argued in the text that this band contains unresolved contributions from two recombination mechanisms, the minor higher-energy one being stronger for high [Au] and at high excitation density. The near-gap luminescence is comparable to Fig. 12.

ABE spectra in Sec. III C is supported by comparison of the optical properties of the single bound hole at Ag_{Zn} , Au_{Zn} , and Cu_{Zn} given from Figs. 5 and 13 of the present paper and Fig. 5 of Dean.⁴⁰ This comparison also shows that the broad red spectra of ZnSe:Ag and ZnSe:Cu are distinctly different, removing any suspicion that Cu may have been introduced inadvertently in attempts to dope with Au. The correctness of the distant DAP identification of the red Cu-related band in ZnSe has been recently confirmed by optically detected magnetic resonance.⁴¹ The same technique has been used to identify a generally less prominent, featureless green luminescence band with distant pair recombinations involving an axial, neutral associate, containing Cu_{Zn} and a donor, possibly Cu_i , and a distant shallow donor.⁴² Thus, a general consensus is appearing which seems consistent with the interpretations for the optical properties of ZnSe:Ag and ZnSe:Au presented in this paper.

We can obtain an estimate of $(E_A)_{\text{Au}}$ from the Arrhenius plot of the temperature dependence of the total intensity also shown in Fig. 10. The thermal activation energy near the high-temperature limit, above 400 K, is $E_A \sim 550$ meV. This might be expected to be a little less than $(E_A)_{\text{Au}}$ because of impurity banding through shallow excited states, probably also responsible for the difference noted for Ag (Sec. III B). This value puts $E_G - E_A$ close to 2.27 eV, near the high-energy limit of the low-temperature spectra in Figs. 12 and 13. The spectrum from the more heavily Au-doped crystal showed a broader luminescence band with an overall high-energy threshold near 2.45 eV, particularly when intensely pumped by strongly absorbed radiation. This is believed due to a second broad band poorly resolved from the lower-energy band dominant under low-density excitation as in Fig. 12. The second band makes a more significant contribution even for the lower-doped sample under intense CL excitation at intermediate temperatures (Fig. 13). This band may result from distant pair recombinations involving Au-donor associate hole traps, the analog of the green Cu band in ZnSe , but involving substitutional donor species according to the arguments of Sec. III A.

The Au-induced absorption was too weak to be clearly substantiated in PLE spectra obtained by lamp and monochromator. Very diffuse structure was seen down to ~ 2.55 eV, again roughly as expected for $E_G - E_A + n\hbar\omega_{\text{LO}}$ where n represents the order of phonon coupling at which significant phonon-assisted absorption might be anticipated. These PLE spectra again showed the broad thresh-

old near 2.76 eV present in Figs. 6 and 7, but significantly *without* the second threshold near 2.774 eV. This is a most interesting observation in view of the tentative attribution of the higher-energy feature to photoionization processes involving the Ag-associate hole trap (Sec. III B).

E. Resonant excitation of Li ABE luminescence

Initial survey measurements made with photographic plates of many of the LPE layers and high-quality vapor-transport samples of ZnSe available showed many cases of strong I_1^x lines, near 2.7925 eV (Table I). These have been attributed to BE recombination at neutral Li acceptors as a result of careful doping studies.²² However, the center responsible for this BE is evidently a very persistent contaminant of refined ZnSe . Positive identification of the chemical origin of such features is notoriously problematical for semiconductor analysis. Thus, more specific methods of verification are particularly welcome for such persistent features. Line-intensity variations in the survey spectra suggested that a component 46.8 meV below I_1^x was closely related to it in intensity, like the component displaced 31.8 meV below due to a recombination event in which an $\text{LO}(\Gamma)$ phonon is created (Table II). Since no electronic satellites of the Li acceptor are expected to have such a small energy,³⁵ it is natural to believe that this satellite might involve a local mode phonon, probable since $M_{\text{Li}} \ll M_{\text{Zn}}$. Indeed, taking an average lattice optical phonon energy $\hbar\omega_0$ of 28.4 meV for ZnSe , the local mode frequency for Li_{Zn}^7 predicted from a simple ball and spring model with unaltered force constants⁴³ is

$$\hbar\omega_{\text{loc}} = \left[\frac{\frac{1}{M_{\text{Li}}} + \frac{1}{4M_{\text{Se}}}}{\frac{1}{M_{\text{Zn}}} + \frac{1}{M_{\text{Se}}}} \right]^{1/2} \hbar\omega_0. \quad (4)$$

Equation (4) predicts $\hbar\omega_{\text{loc}} = 64.8$ meV for ^7Li , so that an appreciable reduction in the force constant of the Li—Se bond compared with Zn—Se must occur to reduce this value to the observed 46.8 meV. In fact, such reductions are commonly observed for small size substituent atoms such as Li.⁴⁴

Clear proof of this assignment of the 46.8-meV satellite is offered by high-sensitivity measurements using SPL of the I_1^x line possible with the dye

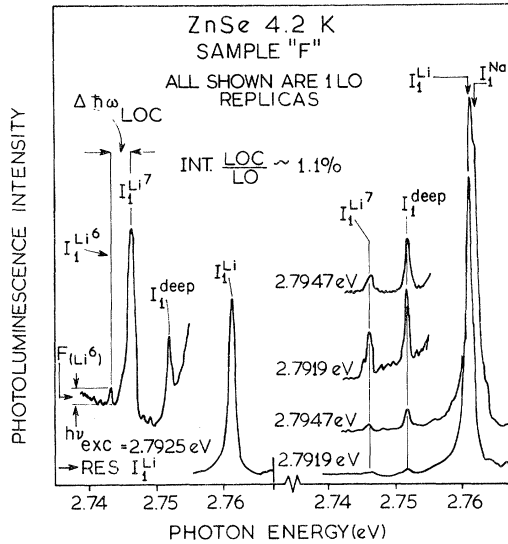


FIG. 14. Portions of the low-temperature photoluminescence of an undoped LPE single crystal of ZnSe containing residual shallow Li and Na acceptors under resonant dye-laser excitation within the neutral ABE no-phonon absorption lines introduced by these species. Only the LO-phonon replicas and associated local modes are seen, including the LO replica of the I_1^{deep} ABE believed to involve the deep Cu acceptor. As the dye laser is tuned from 2.7919 eV, just below peak resonance with I_1^{Li} , to 2.7947 eV, resonant with I_1^{Na} , the contribution of the Na ABE to the combined, incompletely resolved LO-phonon replica increases greatly, as expected. I_1^{deep} and the local mode $I_1^{7\text{Li}}$ are unaffected in line shape, since any local mode due to Na_{Zn} will be well removed from that due to Li_{Zn} . The spectra at the left, recorded under exact resonance with I_1^{Li} , contains an improved intensity ratio $I_1^{\text{Li}}/I_1^{\text{deep}}$. A weak further component consistent with the isotope ${}^6\text{Li}$ in natural abundance is also detected.

laser. Then, the satellites associated with the I_1^{Li} ABE are sufficiently enhanced that a very weak additional satellite displaced 50.0 meV below I_1^{Li} becomes clearly visible above the background luminescence due to discrete DAP and acoustic phonon BE satellites (Fig. 14). The observed change in frequency of 3.2 meV is in very good agreement with the predicted value.

Equation (1) predicts $\Delta\hbar\omega_{\text{loc}} = 3.3$ meV if the new satellite is attributed to the ${}^6\text{Li}$ isotope. This attribution is strongly supported by the good agree-

ment between the observed intensity ratio of $9 \pm 1\%$ between the 50.0- and 46.8-meV satellites and the natural-isotope-abundance fraction $F({}^6\text{Li})$ of 7.4%. Equation (1) is normally expected to give close agreement with an observed isotope shift, since it depends only upon the plausible assumption of the applicability of an harmonic oscillator model with force constants which are independent of the mass of the impurity isotope. The intensity of the ${}^6\text{Li}$ satellite is only $\sim 1.1 \times 10^{-4}$ of that of I_1^{Li} .

The isotope effects in Fig. 14 offer the most intimate proof possible that Li is really the persistent shallow acceptor responsible for the I_1^{Li} ABE in ZnSe. Observation of only a single local mode for each Li also suggests that the Li_{Zn} possesses the full T_d symmetry of the Zn lattice site, consistent with the detailed no-phonon structure of the shallow DAP spectra believed to involve the Li_{Zn} acceptor.²² It is interesting to note that isotope studies on persistent shallow acceptor states in CdS have also revealed the involvement of Li.⁴⁵ Henry *et al.*⁴⁵ demonstrated isotope shifts in no-phonon DAP transitions. These became very small in the limit of small R in Eq. (3), as the DAP recombinations tended to the Be limit. The shifts were unmeasurable for the Li neutral ABE, because of the extra hole which screened out the effects of the isotope mass change in both the initial and final states of the neutral ABE recombination. Detection of a true local mode as a sideband is not subject to this limitation. Tentative identification of a similar type of local mode involving the shallow Na_{Cd} acceptor has been recently obtained in CdSe.⁶⁴ This assignment was not substantiated by isotope shift measurements, but the agreement between the calculated and observed values of the LVM energy was much closer for this larger substantial ion.

ACKNOWLEDGMENTS

The authors are grateful to M. S. Skolnick, P. Porteous, T. McGee, S. Herko, W. Seemungal, A. D. Pitt, and J. Soole for assistance with various aspects of the experimental work.

¹M. D. Ryall and J. W. Allen, *J. Phys. Chem. Solids* **34**, 2137 (1973); J. W. Allen, *J. Luminesc.* **7**, 228 (1973).

²See special issue on high-field electroluminescence, *J. Lumin.* **23**, 1 (1981).

³K. Kosai, B. J. Fitzpatrick, H. G. Grimmeiss, R. N. Bhargava, and G. F. Neumark, *Appl. Phys. Lett.* **35**, 194 (1979).

⁴K. Era, S. Shionoya, and Y. Washizawa, *J. Phys.*

- Chem. Solids **29**, 1827 (1968).
- ⁵K. Schwenkenbecher, R. Boyn, and H. Resaqk, Phys. Status Solidi B **101**, 215 (1980).
- ⁶L. A. Hemstreet, Phys. Rev. B **22**, 4590 (1980).
- ⁷H. A. Weakliem, J. Chem. Phys. **36**, 2117 (1962).
- ⁸D. C. Herbert, P. J. Dean, H. Venghaus, and J. C. Pfister, J. Phys. C **11**, 3641 (1978).
- ⁹N. Magnea, D. Bensahel, J. L. Pautrat, and J. C. Pfister, Phys. Status Solidi B **94**, 627 (1979).
- ¹⁰H. Venghaus and P. J. Dean, Phys. Rev. B **21**, 1596 (1980).
- ¹¹D. J. Robbins and P. J. Dean, Adv. Phys. **27**, 499 (1978).
- ¹²B. J. Fitzpatrick, C. J. Werkhoven, T. F. McGee III, P. M. Harnack, S. P. Herko, R. N. Bhargava, and P. J. Dean, IEEE Trans. Electron Devices **ED-28**, 440 (1981).
- ¹³R. E. Dietz, H. Kamimura, M. D. Sturge, and A. Yariv, Phys. Rev. **132**, 1559 (1963).
- ¹⁴M. de Wit, Phys. Rev. **177**, 441 (1969); M. Tabei and S. Shionoya, J. Lumin. **15**, 201 (1977).
- ¹⁵C. Werkhoven, B. J. Fitzpatrick, S. P. Herko, R. N. Bhargava, and P. J. Dean, Appl. Phys. Lett. **38**, 540 (1981).
- ¹⁶P. J. Dean, D. C. Herbert, C. J. Werkhoven, B. J. Fitzpatrick, and R. N. Bhargava, Phys. Rev. B **23**, 4888 (1981).
- ¹⁷D. J. Robbins, B. Cockayne, J. L. Glasper, and B. Lent, J. Electrochem. Soc. **126**, 1213 (1979).
- ¹⁸J. L. Merz, H. Kukimoto, K. Nassau, and J. W. Shiever, Phys. Rev. B **6**, 545 (1972).
- ¹⁹V. Swaminathan and L. C. Greene, J. Lumin. **14**, 357 (1976).
- ²⁰P. J. Dean and D. C. Herbert, in *Excitons*, Vol. 14 of *Topics in Current Physics*, edited by K. Cho (Springer, Berlin, 1979), p. 55.
- ²¹B. Hennion, F. Moussa, G. Pepy, and K. Kunc, Phys. Lett. **36A**, 376 (1971).
- ²²J. L. Merz, K. Nassau, and J. W. Shiever, Phys. Rev. B **8**, 1444 (1973).
- ²³C. H. Henry, P. J. Dean, and J. D. Cuthbert, Phys. Rev. **166**, 754 (1968); C. H. Henry, P. J. Dean, D. G. Thomas, and J. J. Hopfield, in *Proceedings of the Conference on Localized Excitations in Solids*, edited by R. F. Wallis (Plenum, New York, 1968), p. 267.
- ²⁴A. Grimm, A. A. Maradudin, I. P. Ipatova, and A. V. Subashiev, J. Phys. Chem. Solids **33**, 775 (1972).
- ²⁵P. J. Dean, B. Monemar, H. P. Gislason, and D. C. Herbert, J. Lumin. **24-25**, 401 (1981).
- ²⁶D. J. Ashen, P. J. Dean, D. T. J. Hurle, J. B. Mullin, A. M. White, and P. D. Greene, J. Phys. Chem. Solids **36**, 1041 (1975).
- ²⁷P. J. Dean, in *Progress in Solid State Chemistry*, edited by J. O. McCaldin and G. Somorjai (Pergamon, New York, 1973), Vol. 8, p. 1.
- ²⁸W. Schmid and P. J. Dean, Phys. Status Solidi B **110**, 591 (1982).
- ²⁹M. O. Henry, E. C. Lightowers, N. Killoran, D. J. Dunstan, and B. C. Cavenett, J. Phys. C **14**, L255 (1981).
- ³⁰A. M. White, P. J. Dean, K. M. Fairhurst, W. Bardsley, and B. Day, J. Phys. C **7**, L35 (1974).
- ³¹B. V. Dutt and W. G. Spitzer, J. Appl. Phys. **47**, 573 (1976).
- ³²E. Cohen and M. D. Sturge, Phys. Rev. B **15**, 1039 (1977).
- ³³H. Tews and H. Venghaus, Solid State Commun. **30**, 219 (1979).
- ³⁴H. Venghaus, P. J. Dean, P. E. Simmonds, and J. C. Pfister, Z. Phys. B **30**, 125 (1978).
- ³⁵T. Suda, K. Matsuzaki, and S. Kurita, J. Appl. Phys. **50**, 3638 (1979).
- ³⁶N. Magnea, J. L. Pautrat, K. Saminadayar, B. Pajot, P. Martin, and A. Bontemps, Rev. Phys. Appl. **15**, 701 (1980).
- ³⁷R. H. Bube and E. L. Lind, Phys. Rev. **110**, 1040 (1958).
- ³⁸R. E. Halsted, M. Aven, and H. D. Coghill, J. Electrochem. Soc. **112**, 177 (1965).
- ³⁹J. W. Allen, P. J. Dean, and A. M. White, J. Phys. C **9**, L113 (1976).
- ⁴⁰P. J. Dean, Czech. J. Phys. B **30**, 272 (1980).
- ⁴¹M. Godlewski, W. E. Lamb, and B. C. Cavenett, Solid State Commun. **39**, 595 (1981).
- ⁴²J. L. Patel, J. J. Davies, and J. E. Nicholls, J. Phys. C **14**, 5545 (1981).
- ⁴³D. G. Thomas and J. J. Hopfield, Phys. Rev. **160**, 680 (1966).
- ⁴⁴P. J. Dean, Phys. Rev. B **4**, 2596 (1971).
- ⁴⁵C. H. Henry, K. Nassau, and J. W. Shiever, Phys. Rev. B **4**, 2453 (1971).
- ⁴⁶N. Magnea, D. Bensahel, J. L. Pautrat, K. Saminadayar, and J. C. Pfister, Solid State Commun. **30**, 259 (1979).
- ⁴⁷G. Neu, Y. Marfaing, R. Legros, R. Triboulet, and L. Svob, J. Lumin. **21**, 293 (1980).
- ⁴⁸G. Neu, R. Legros, Y. Marfaing, J. F. Rommeluere, and R. Triboulet, J. Electrochem. Soc. **128**, 239C (1981).
- ⁴⁹A. R. Reinberg, W. G. Holton, M. deWit, and R. K. Watts, Phys. Rev. B **3**, 410 (1971).
- ⁵⁰K. M. Lee, Le Si Dang, and G. D. Watkins, Solid State Commun. **35**, 527 (1980).
- ⁵¹J. C. Bouley, P. Blanconnier, A. Herman, Ph. Ged, P. Henoc, and J. P. Noblanc, J. Appl. Phys. **46**, 3549 (1975); D. J. Dunstan, J. E. Nicholls, B. C. Cavenett, and J. J. Davies, J. Phys. C **13**, 6409 (1980).
- ⁵²J. L. Pautrat, E. Molva, N. Magnea, and J. C. Pfister, in *Proceedings of the International Conference on Radiation Defects in Semiconductors, Tokyo, 1980* (Institute of Physics, London, 1981).
- ⁵³A. Suzuki and S. Shionoya, J. Phys. Soc. Jpn. **31**, 1455 (1971); **31**, 1462 (1971).
- ⁵⁴S. Gezci and J. Woods, J. Appl. Phys. **51**, 1866 (1980).
- ⁵⁵H. G. Grimmeiss, N. Kullendorff, and R. Broser, J.

- Appl. Phys. 52, 3405 (1981).
- ⁵⁶G. D. Watkins, Solid State Commun. 12, 589 (1973).
- ⁵⁷H. G. Grimmeiss, C. Ovren, and R. Mach, J. Appl. Phys. 50, 6328 (1979).
- ⁵⁸G. Muller, Phys. Status Solidi B 76, 525 (1976).
- ⁵⁹O. F. Schirmer and D. Zwingel, Solid State Commun. 8, 1559 (1970).
- ⁶⁰D. Zwingel and F. Gartner, Solid State Commun. 14, 45 (1974).
- ⁶¹M. A. Rizakhanov, Yu N. Emirov, F. S. Galibov, M. M. Khamidov, and M. K. Sheinkman, Fiz. Tekh. Poluprovodn. 12, 1342 (1978) [Sov. Phys.—Semicond. 12, 794 (1978)].
- ⁶²W. Czaja and A. Baldereschi, J. Phys. C 12, 405 (1979).
- ⁶³H. Tews, H. Venghaus, and P. J. Dean, Phys. Rev. B 19, 5178 (1979).
- ⁶⁴P. Y. Yu and C. Hermann, Phys. Rev. B 23, 4097 (1981).